

Field-Induced Spin Nematic Liquid of the $S = 1/2$ Bond-Alternating Chain with the Anisotropy

Ryosuke NAKANISHI¹, Takaharu YAMADA¹, Rito FURUCHI¹, Hiroki NAKANO¹,
Hirono KANEYASU¹, Kiyomi OKAMOTO¹, Takashi TONEGAWA^{1,2,3}, and
Tôru SAKAI^{1,4}

¹*Graduate School of Science, University of Hyogo, Hyogo 678-1297, Japan*

²*Professor Emeritus, Kobe University, Kobe 657-8501, Japan*

³*Department of Physics, Graduate School of Science, Osaka Metropolitan University, Sakai, Osaka 599-8531, Japan*

⁴*National Institutes for Quantum Science and Technology (QST), SPring-8, Hyogo 679-5148, Japan*

E-mail: ryosukenakanishi7@gmail.com

(Received July 12, 2022)

The $S = 1/2$ ferromagnetic-antiferromagnetic bond-alternating spin chain with the anisotropy on the ferromagnetic exchange interaction in magnetic field is investigated using the numerical diagonalization and the density matrix renormalization group analyses. It is found that the nematic-spin-dominant Tomonaga-Luttinger liquid phase is induced by the external magnetic field for sufficiently large anisotropy. The phase diagram with respect to the anisotropy and the magnetization is presented.

KEYWORDS: quantum spin system, spin nematic liquid, quantum spin liquid, quantum phase transition

1. Introduction

The spin nematic order [1, 2] is one of interesting topics in the field of the low-temperature physics. It is the long-range quadrupole order of spins by forming the two-magnon bound state. It is a kind of an intermediate state between the conventional long-range magnetic order and the quantum spin liquid. The previous theoretical mechanisms of the spin nematic order have been based on the biquadratic exchange interaction [3–9] which directly stabilizes the nematic correlation, or the spin frustration [10–19] which suppresses the conventional long-range order. We note that we showed the existence of the spin nematic liquid phase under zero magnetic field in a model having neither the biquadratic interaction nor the frustration [20]. Also we found the spin nematic liquid phase under magnetic field in several one-dimensional models [21–25]. In this paper we propose a simple model that possibly exhibits the spin nematic liquid phase in magnetic field without the biquadratic interaction or the frustration. Our present model is the $S = 1/2$ ferromagnetic-antiferromagnetic bond-alternating spin chain with the Ising-like coupling anisotropy at the ferromagnetic bond. When the external magnetic field is applied to this system, the gapless Tomonaga-Luttinger liquid (TLL) phase is expected to be realized. The present numerical diagonalization analysis indicates that the conventional TLL (CTLL) phase would change to another TLL phase where the quasiparticle is the two-magnon bound state for sufficiently large anisotropy. The present analysis of the critical exponents of some spin correlation functions reveals that the nematic-spin-correlation dominant TLL region appears in the two-magnon TLL phase. A typical phase diagram with

respect to the anisotropy and the magnetization is presented.

2. Model

We consider the magnetization process of the $S = 1/2$ ferromagnetic-antiferromagnetic bond-alternating spin chain with the Ising-like coupling anisotropy at the ferromagnetic bond. The Hamiltonian is given by

$$\mathcal{H} = \mathcal{H}_0 + \mathcal{H}_Z, \quad (1)$$

$$\mathcal{H}_0 = J_1 \sum_{j=1}^L \left[S_{2j-1}^x S_{2j}^x + S_{2j-1}^y S_{2j}^y + \lambda S_{2j-1}^z S_{2j}^z \right] + J_2 \sum_{j=1}^L \mathbf{S}_{2j} \cdot \mathbf{S}_{2j+1} \quad (2)$$

$$\mathcal{H}_Z = -H \sum_{j=1}^L (S_{2j-1}^z + S_{2j}^z), \quad (3)$$

where λ is a coupling anisotropy parameter and H is the external magnetic field along the z direction. The ferromagnetic interaction constant J_1 is set to -1 . We consider the case in which $J_2 > 0$ (antiferromagnetic) and the anisotropy of the J_1 bond is Ising-like ($\lambda > 1$). For the length L system, the lowest energy of \mathcal{H}_0 in the subspace $\sum_j S_j^z = M$ is denoted by $E(L, M)$. The reduced magnetization m is defined by $m = M/M_s$, where M_s denotes the saturation of the magnetization, namely $M_s = L$. The energy $E(L, M)$ is calculated by the Lanczos algorithm under the periodic boundary condition ($\mathbf{S}_{2L+1} = \mathbf{S}_1$). Our calculation of the magnetization curve indicates that for $J_2 \gtrsim |J_1|$ the spin nematic liquid phase does not appear, because the magnetization jump like the spin flop occurs. Thus in this paper we fix J_2 to 0.3, which is a typical case where the spin nematic liquid appears clearly.

3. Ground State without Magnetic Field

The ground state of the ferromagnetic and antiferromagnetic bond-alternating chain without magnetic field is in the Haldane phase when $\lambda = 1$, whereas it would be in the Néel ordered phase for sufficiently large λ . The phase boundary between these two phases can be estimated with the phenomenological renormalization [26]. The size-dependent phase boundary is estimated by the fixed point equation for the two system sizes L and $L + 2$

$$L\Delta_\pi(L, \lambda) = (L + 2)\Delta_\pi(L + 2, \lambda), \quad (4)$$

where Δ_π is the excitation gap with $k = \pi$ in the subspace with $M = 0$. The scaled gap $L\Delta_\pi$ is plotted versus λ for $L = 8, 10, 12, 14$ in Fig. 1. It suggests that the phase boundary exists around $\lambda \sim 1.17$. The extrapolation of the size-dependent fixed point $\lambda_c(L + 1)$ for L and $L + 2$ assuming the size correction proportional to $1/(L + 1)$, as shown in Fig. 2, results in $\lambda_c = 1.172 \pm 0.001$ in the infinite length limit.

4. Two Tomonaga-Luttinger Liquids

In the magnetization process for $\lambda = 1$ the system is in the CTLL phase for $0 < m < 1$. In the strong J_1 limit the spin pair on the J_1 bond forms the triplet with three states $|\uparrow\uparrow\rangle$, $(|\uparrow\downarrow\rangle + |\downarrow\uparrow\rangle)/\sqrt{2}$ and $|\downarrow\downarrow\rangle$. For sufficiently large λ two states $|\uparrow\uparrow\rangle$ and $|\downarrow\downarrow\rangle$ are stabilized and the remaining state $(|\uparrow\downarrow\rangle + |\downarrow\uparrow\rangle)/\sqrt{2}$ is excluded in the magnetization process. As a result the two-magnon bound state is realized and each magnetization step is not $\delta M=1$ but

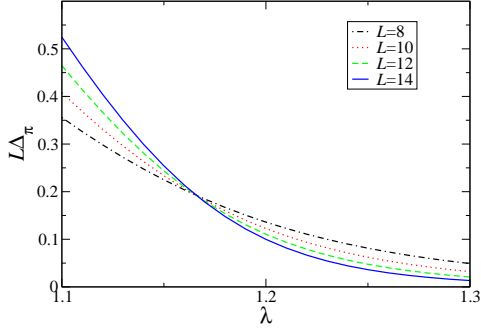


Fig. 1. Scaled gap $L\Delta_\pi$ is plotted versus λ for $L = 8, 10, 12, 14$ when $m = 0$.

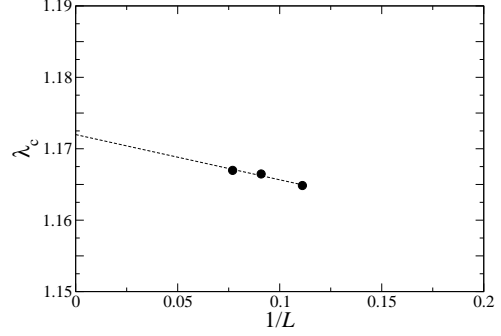


Fig. 2. Extrapolation of the size-dependent fixed point $\lambda_c(L+1)$ for L and $L+2$ assuming the size correction proportional to $1/(L+1)$. It results in $\lambda_c = 1.172 \pm 0.001$ in the infinite length limit.

$\delta M=2$. This large λ phase is also a kind of TLL phase, but different from the CTLL phase. We call it the two-magnon TLL (TMTLL) phase. Now we consider three excitation gaps; they are the single-magnon excitation gap Δ_1 , the two-magnon excitation gap Δ_2 , and the $2k_F$ excitation gap in the TMTLL phase Δ_{2k_F} . In both TLL phases Δ_2 is gapless. In contrast, Δ_1 (Δ_{2k_F}) is gapless (gapped) in the CTLL phase, but is gapped (gapless) in the TMTLL one. For $m = 1/2$ the scaled gaps $L\Delta_1$, $L\Delta_2$ and $L\Delta_{2k_F}$ are plotted versus λ for $L = 8$ and 12 in Fig. 3. The gapless and gapped behaviors of these excitations mentioned above are confirmed in Fig. 3. The finite-size effect of the fixed points are shown in Fig. 4. The fixed points of Δ_1 and Δ_{2k_F} behave as $1/L^2$, whereas those of Δ_1 and Δ_2 as $1/L$. Unfortunately it is impossible to perform such extrapolations for general m . Thus we use the cross point of Δ_1 and Δ_{2k_F} for largest L as the phase boundary between the two TLL phases at each m , which leads the difficulty in obtaining accurate boundary. The error of the estimated boundary can be surmised from Fig. 4.

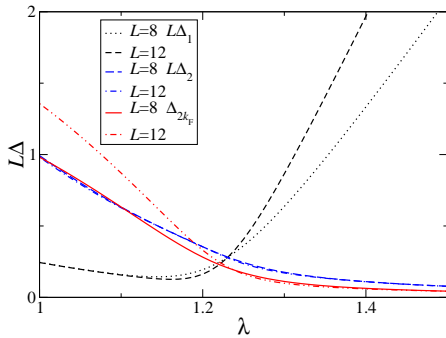


Fig. 3. Scaled gaps $L\Delta_1$, $L\Delta_2$ and $L\Delta_{2k_F}$ are plotted versus λ for $L = 8$ and 12 for $m = 1/2$.

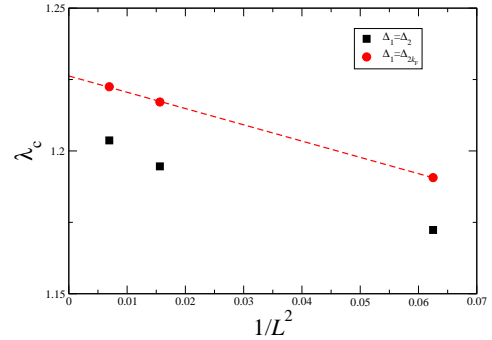


Fig. 4. Extrapolation of the size-dependent fixed points λ_c of $L\Delta_1$ and $L\Delta_2$ (black squares), and those of $L\Delta_1$ and $L\Delta_{2k_F}$ (red circles). By use of the latter points, it results in $\lambda_c = 1.2262 \pm 0.0003$ in the infinite length limit.

5. Spin-Density-Wave and Nematic Spin Correlations

The quasi-long-range spin-density-wave (SDW) and nematic orders are expected to appear in the TMTLL phases. They are characterized by the power-law decays of the following spin correlation functions

$$\langle S_1^z S_{2r+1}^z \rangle - \langle S^z \rangle^2 \sim \cos(2k_F r) r^{-\eta_z}, \quad (5)$$

$$\langle S_1^+ S_2^+ S_{2r+1}^- S_{2r+2}^- \rangle \sim r^{-\eta_2}. \quad (6)$$

Here Eq.(5) corresponds to the SDW spin correlation parallel to the external field and Eq.(6) corresponds to the nematic spin correlation perpendicular to the external field. The smaller exponent between η_z and η_2 determines the dominant spin correlation. According to the conformal field theory these exponents can be estimated by the forms

$$\eta_2 = \frac{E(L, M+2) + E(L, M-2) - 2E(L, M)}{E_{k_1}(L, M) - E(L, M)}, \quad (7)$$

$$\eta_z = 2 \frac{E_{2k_F}(L, M) - E(L, M)}{E_{k_1}(L, M) - E(L, M)}, \quad (8)$$

for each magnetization M , where k_1 is defined as $k_1 = L/2\pi$. The exponents η_2 and η_z estimated for $L = 12$ and 14 are plotted versus m for $\lambda = 1.3$ in Fig.5. Since the system size dependence of η_2 is smaller than that of η_z , we estimate the crossover point between the SDW dominant and the spin nematic dominant TLL phases as the point $\eta_2 = 1$, assuming the relation $\eta_z \eta_2 = 1$ which should be satisfied in the TMTLL TLL phase.

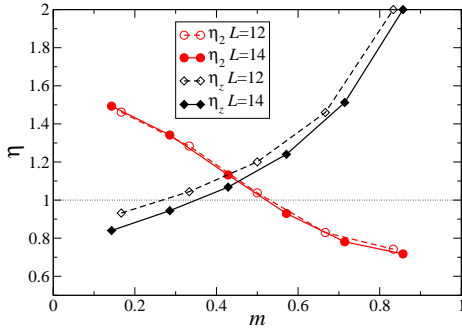


Fig. 5. Exponents η_2 and η_z estimated for $L = 12$ and 14 are plotted versus m for $\lambda = 1.3$.

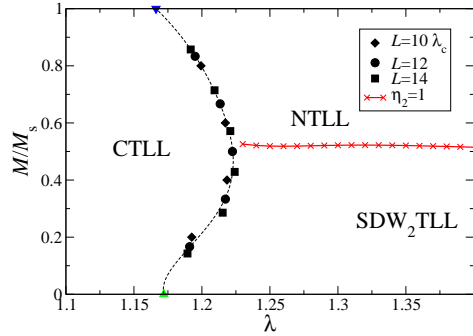


Fig. 6. Phase diagram on the $\lambda - m$ plane for $J_2 = 0.3$. CTLL, SDW₂TLL and NTLL correspond to the conventional TLL, the SDW correlation dominant TLL and the spin nematic correlation dominant TLL phases, respectively.

6. Phase Diagram and Magnetization Curve

The phase diagram with respect to the anisotropy λ and the magnetization for $J_2 = 0.3$ is shown in Fig. 6. The boundary between the CTLL and the TMTLL phases is estimated by $\Delta_1 = \Delta_{2k_F}$ for $L = 10, 12$ and 14 . The crossover line between the spin-nematic dominant TLL (NTLL) and the SDW dominant TLL (SDW₂TLL) phases is estimated by $\eta_2 = 1$. We note that the TMTLL phase is composed of the NTLL phase and the SDW₂TLL phase.

The phase diagram indicates that the magnetization process for $\lambda \sim 1.2$ would meet two field-induced quantum phase transitions; one is between the SDW₂TLL and CTLL phases, the other is between the CTLL and NTLL ones. The magnetization curve calculated by the density matrix renormalization group (DMRG) for $L = 48$ and $\lambda = 1.2$ is shown in Fig. 7. Since each magnetization step is $\delta M=1$ in the CTLL phase and $\delta M=2$ in the SDW₂TLL and NTLL regions, the two transitions are confirmed to occur.

7. Discussion and Summary

The mechanism for the appearance of the TMTLL phase in this model has been explained in §2. We think that the mechanisms are essentially the same for our previous the models [21–25]. For instance, in the $S = 1$ models [22–24], two states $|S^z = \pm 1\rangle$ of an $S = 1$ spin are selected by the anisotropy effect, which is directly seen from the Hamiltonian. This is very similar to the mechanism of the present model, because $1 - \lambda$ of the present model corresponds to the on-site anisotropy (so-called D parameter) of the $S = 1$ model. The TMTLL phase also appeared under the magnetic field in the $S = 1/2$ chain model with the nearest-neighbor ferromagnetic and the next-nearest-neighbor antiferromagnetic interactions (NNF-NNNAF model) [18, 19]. The situation seems to be quite different in the NNF-NNNAF model, because such a selection of states cannot be seen from the properties of the Hamiltonian itself. We think that the appearance of the TMTLL phase in the NNF-NNNAF model is due to the combined many-body effect of the frustration and the magnetic field. This reminds us that the dimerized state is realized in both of the $S = 1/2$ bond-alternating antiferromagnetic chain [27] and the $S = 1/2$ antiferromagnetic chain with the next-nearest-neighbor interactions [28, 29]. Their mechanisms are quite different from each other. The former is explained by the bond-alternating nature of the Hamiltonian itself, whereas the latter by the many-body effect originated from the frustration.

From the phase diagram Fig.6, for $\lambda = 1.2$, we can estimate the lower critical field for the SDW₂TLL-CTLL boundary as $m_{c1} = 0.214$ and the upper one for the CTLL-NTLL boundary as $m_{c2} = 0.795$. While, from Fig. 7, we obtain $m_{c1} = 0.208$ and $m_{c2} = 0.708$. The considerable difference in m_{c2} may come from the method of the estimation of the phase boundary by spin gaps (as we stated, the size extrapolation is impossible in principle), and also the steep curves of the phase boundary and the magnetization near m_{c2} . From the discussion on the behavior of correlation functions, we said that the CTLL-TMTLL boundary can be determined by $\Delta_1 = \Delta_2$ or $\Delta_1 = \Delta_{2k_F}$ (actually we used the latter for drawing the phase diagram). On the other hand, the condition for the change of the magnetization step between $\delta M = 1$ and $\delta M = 2$ is $2\Delta_1 = \Delta_2$, which is different from the above condition $\Delta_1 = \Delta_2$. This seeming contradiction can be resolved as follows. Since $\eta_2 = 4\eta_1$ in the CTLL phase [19], the ratio of the spin gaps Δ_2/Δ_1 is 4 in the limit of $L \rightarrow \infty$. In the TMTLL phase, Δ_1 is gapped and Δ_2 behaves as $1/L$, which leads to $\Delta_2/\Delta_1 = 0$ in the limit of $L \rightarrow \infty$. Thus, Δ_2/Δ_1 jumps from 4 to 0 at the CTLL to TMTLL transition point in this limit. Therefore both of the condition

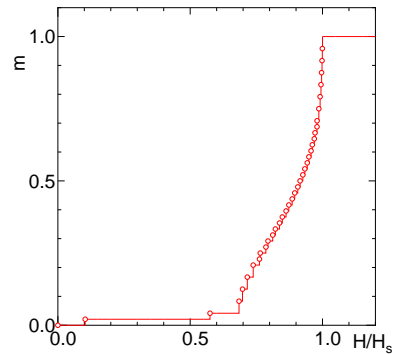


Fig. 7. Magnetization curve calculated by the DMRG for $L = 48$, $J_2 = 0.3$ and $\lambda = 1.2$. Here H_s is the saturation magnetic field. We can see that the magnetization step is $\delta M = 2$ in the low magnetization region, $\delta M = 1$ in the intermediate magnetization region, and again $\delta M = 2$ in the high magnetization region.

$\Delta_1 = \Delta_2$ and $2\Delta_1 = \Delta_2$ converge into the same CTLL to TMTLL transition point in the thermodynamical limit.

In summary, the $S = 1/2$ ferromagnetic and antiferromagnetic bond-alternating chain with the coupling anisotropy at the ferromagnetic bond is investigated using the numerical diagonalization. For sufficiently large Ising-like anisotropy the field-induced NTLL phase appears as well as the SDW₂TLL one. The phase diagram with respect to the anisotropy and the magnetization for a typical parameter is presented. The behavior of the magnetization curve by the DMRG is consistent with the phase diagram.

Acknowledgment

This work has been partly supported by JSPS KAKENHI, Grant Numbers 16K05419, 16H01080 (J-Physics), 18H04330 (J-Physics), JP20K03866, and JP20H05274. We also thank the Supercomputer Center, Institute for Solid State Physics, University of Tokyo and the Computer Room, Yukawa Institute for Theoretical Physics, Kyoto University for computational facilities. We have also used the computational resources of the supercomputer Fugaku provided by the RIKEN through the HPCI System Research projects (Project ID: hp200173, hp210068, hp210127, hp210201, and hp220043).

References

- [1] A. F. Andreev and A. Grishchuk, Sov. Phys. JETP **60**, 267 (1984).
- [2] H. H. Chen and P. M. Levy, Phys. Rev. Lett. **27**, 1383 (1971).
- [3] A. V. Chubukov, J. Phys.: Condens. Matter **2**, 1593 (1990).
- [4] G. Fáth and J. Sólyom, Phys. Rev. B **51**, 3620 (1995).
- [5] A. Läuchli, G. Schmid and S. Trebst, Phys. Rev. B **74**, 144426 (2006).
- [6] T. Grover and T. Senthil, Phys. Rev. Lett. **98**, 247202 (2007).
- [7] S. R. Manmana, A. Läuchli, F. H. Essler and F. Mila, Phys. Rev. B **83**, 184433 (2011).
- [8] R. M. Mao, Y.-W. Dai, S. Y. Cho and H.-Q. Zhou, Phys. Rev. B **103**, 014446 (2021).
- [9] Y. A. Fridman, O. A. Kosmachev, A. K. Kolezhuk and B. A. Ivanov, Phys. Rev. Lett. **106**, 097202 (2011).
- [10] P. Chandra and P. Coleman, Phys. Rev. Lett. **66**, 100 (1991).
- [11] S. Nakatsuji, Y. Nambu, H. Tonomura, O. Sakai, S. Jonas, C. Broholm, H. Tsunetsugu, Y. Qiu and Y. Maeno, Science **309**, 1697 (2005).
- [12] H. Tsunetsugu and M. Arikawa, J. Phys. Soc. Jpn. **75**, 083701 (2006).
- [13] A. Läuchli, F. Mila and K. Penc, Phys. Rev. Lett. **97**, 087205 (2006).
- [14] S. Bhattacharjee, V. B. Shenoy and T. Senthil, Phys. Rev. B **74**, 092406 (2006).
- [15] J.-H. Park, S. Onoda, N. Nagaosa and J. H. Han, Phys. Rev. Lett. **101**, 167202 (2008).
- [16] A. V. Chubukov, Phys. Rev. B **44**, 4693 (1991).
- [17] T. Vekua, A. Honecker, H.-J. Mikeska and F. Heidrich-Meisner, Phys. Rev. B **76**, 174420 (2007).
- [18] J. Sudan, A. Lüscher, and A. M. Läuchli, Phys. Rev. B **80**, 140402(R) (2009).
- [19] T. Hikihara, L. Kecke, T. Momoi and A. Furusaki, Phys. Rev. B **78**, 144404 (2008).
- [20] T. Tonegawa, T. Hikihara, K. Okamoto, S. C. Furuya, and T. Sakai, J. Phys. Soc. Jpn. **87**, 104002 (2018).
- [21] T. Sakai, T. Tonegawa, and K. Okamoto, Phys. Status Solidi B **247**, 583 (2010).
- [22] T. Sakai and K. Okamoto, JPS Conf. Proc. **30**, 011083 (2020).
- [23] T. Sakai, AIP Advances **11**, 015306 (2021).
- [24] T. Sakai, H. Nakano, R. Furuchi and K. Okamoto, J. Phys.: Conf. Ser. **2164**, 012030 (2022).
- [25] T. Sakai, R. Nakanishi, T. Yamada, R. Furuchi, H. Nakano, H. Kaneyasu, K. Okamoto, and T. Tonegawa, Phys. Rev. B **106**, 064433 (2022).
- [26] P. Nightingale, J. Appl. Phys. **53**, 7927 (1982).
- [27] K. Okamoto and T. Sugiyama, J. Phys. Soc. Jpn. **57**, 1610 (1988).
- [28] C. K. Majumdar and D. K. Ghosh, J. Math. Phys. **10**, 1399 (1969).
- [29] K. Okamoto and K. Nomura, Phys. Lett. A **169**, 437 (1992).